

**Figure 1. (a) Packing density dependence of coercivity at different temperature. Figure 1. (b) SEM micrograph of the Co NW assemblies. The inset image is the Co NW assembly pellet.**

**FJ-12. Local magnetic interactions in Cadmium-doped Cobalt allotropic phases by first principles calculation.** *L.F. Pereira<sup>1</sup> and A.W. Carbonari<sup>1</sup>*  
<sup>1</sup> IPEN, Sao Paulo, Brazil

Cobalt is one of the most attractive ferromagnetic material at room temperature. While Co is used in industrial processes of catalysis, in fundamental science, the connection between the different crystal structure with magnetic properties of Co has attained the attention. Co can crystallize in four different structures: hexagonal closed-packed (hcp, alpha), face-centered cubic (fcc, beta), primitive cubic (epsilon), and body-centered cubic (bcc). The hcp and fcc phases are stable in bulk and nanostructured samples and the difference in their formation energy is small so that, even under small variations of temperature and/or pressure conditions, hcp and fcc can interexchange easily. Often, the literature reports the co-existence of both structures. In last years, new routes of the synthesis and improvement in previous methods have allowed the production of nanostructured Cobalt samples with Epsilon and bcc crystalline phases, which under usual conditions are metastable. The magnetic properties vary with the structure differences in their electronic structure, e.g. the hcp phase has higher coercivity, whereas the fcc is a soft magnet. In the work here reported, first-principles calculations were performed in the four Co structures in order to investigate one sensitive and quite local parameter: the magnetic hyperfine field (mhf). We have used Augmented Planes Waves plus local orbitals (APW+lo) all-electron method based on the density functional theory and implemented in the WIEN2k code to simulate supercells of Co doped with Cd. The resulting mhf at Cd ions is compared with values from perturbed angular correlation spectroscopy measurements using <sup>111</sup>Cd as probe nuclei found in the literature for hcp, fcc, and bcc phases. Up to date, experimental results for mhf at <sup>111</sup>Cd for epsilon structure are not available. Calculated mhf and magnetic moments agree well with reported experimental values - tab. 1. From the calculated density of states for each structure, it is possible to investigate the differences in the magnetic exchange interaction at an atomic view

	Fermi contact magnetic hyperfine field (Tesla)					
	Co site - single cell			Cd@Co site - supercell		
	core	valence	total	core	valence	total
Co-hcp	32.71	-44.26	-11.55	-0.02	10.96	10.94
Co-fcc	26.07	-52.08	-26.01	26.07	-52.08	-26.01
Co-bcc	33.53	-54.48	-20.95	-0.07	-17.07	-17.14
Site Co1	-21.77	-6.20	-27.97	-0.37	-32.48	-32.85
Co-f	-22.93	-3.65	-26.58	-0.21	-25.46	-25.67

**Tab 1. Mhf from Fermi contact component at Co (single cell) and Cd (supercells) sites in the Co allotropic phases. Most important columns are labelled with total**

**FJ-13. Magnetic properties and microstructure of nanocomposite (La,Pr)<sub>3</sub>Fe<sub>14</sub>B ribbons by doping La element.** *Y. Li<sup>1</sup>, S. Peng<sup>1</sup>, M. Zhang<sup>2</sup>, S. Wang<sup>3</sup>, S. Zhu<sup>1</sup>, J. Zhang<sup>4</sup> and F. Shen<sup>1</sup>*  
<sup>1</sup> The State Key Laboratory of Refractories and Metallurgy, Hubei Province Key Laboratory of Systems Science in Metallurgical Process, International Research Institute for Steel Technology, Wuhan University of Science and Technology, Wuhan, China; <sup>2</sup> Faculty of Science, Inner Mongolia University Of Science and Technology, Inner Mongolia, China; <sup>3</sup> Faculty of Science, Northwestern Polytechnical University, Xian, China; <sup>4</sup> Institute of Physics, Chinese Academy of Sciences, Beijing, China

For the scarce resources and high cost of Nd/Pr metal, the doping of rare earth elements (mainly La and Ce) in Nd-Fe-B or Pr-Fe-B iron based permanent magnet material has gradually been a hot research in recent

years, namely, mixed rare earth-iron based permanent magnet compounds. Most researches were focused on La doped Nd-Fe-B [1]. In this paper, we have performed a systematic study on La doped Pr-Fe-B ((La,Pr)<sub>1-x</sub>)<sub>3</sub>Fe<sub>14</sub>B, x=0, 0.3, 0.6, (La,Pr)-Fe-B), focusing on the magnetic properties of (La,Pr)-Fe-B compounds by La doping. We have synthesized (La,Pr)-Fe-B samples by vacuum arc melting technique, and further fabricated (La,Pr)-Fe-B magnetic ribbons through melt-spinning method at the optimized quenching speed of 20m/s[2]. The microstructure, element distribution, magnetic properties, magnetization process of samples were investigated. Figure 1 shows XRD patterns of the samples, showing the effects of La content on microstructure evolution. All the samples present 2:14:1 main phase and α-Fe phase, and the extra La<sub>2</sub>O<sub>3</sub> phase formed in La doped (La,Pr)-Fe-B. EBSD results (not shown) reveal that rare earth-rich phases are mostly distributed over the grain boundary, and samples actually have a higher La/Pr ratio compared with the nominal ratio. The magnetic hysteresis loops of (La,Pr)-Fe-B ribbons show that, the La content has some influence on the coercivity, but little on the saturation magnetization (Fig.2). The results are related with the segregation of La in grain boundary, and the coercivity was identified to be dominated by domain wall pinning mechanism. The magnetization and demagnetization process were studied in the paper. Our results demonstrate the effect of La doping on the structure and magnetic properties of Pr-Fe-B magnet. This work has revealed the relationship between micro-structure and magnetic performance in La doped Pr-Fe-B mixed rare earth-iron based permanent magnet compounds, indicating the feasibility of replacing Pr with La in Pr-Fe-B magnet to achieve low cost and similar magnetic performance.

[1] Z. Li, W. Q. Liu, S. S. Zha et al., J. Rare Earth, 33, 961 (2015). [2] M. Zhang, Z. B. Li, B. G. Shen et al., J. Alloys Comp., 651, 144 (2015).

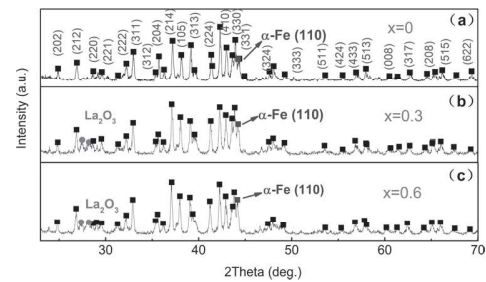


**Fig.1 XRD patterns of (La<sub>x</sub>Pr<sub>1-x</sub>)<sub>3</sub>Fe<sub>14</sub>B samples, (a) x=0, (b) x=0.3, (c) x=0.6.**

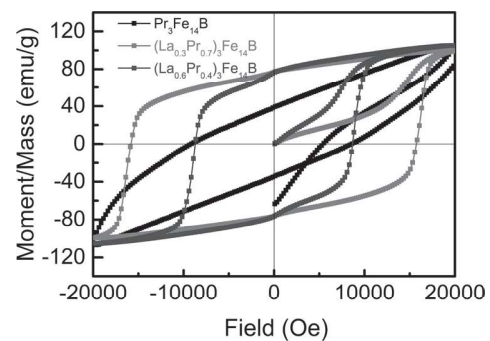


**Fig.2 The magnetic hysteresis loops of (La<sub>x</sub>Pr<sub>1-x</sub>)<sub>3</sub>Fe<sub>14</sub>B (x=0, 0.3, 0.6) ribbons.**